J. Biochem. **143,** 97–105 (2008)
doi:10.1093/jb/mvm197

Reshuffling of the *Bacillus subtilis* 168 Genome by Multifold Inversion

Azusa Kuroki[1,2], Tsutomu Toda[3], Kuniko Matsui[3], Rie Uotsu-Tomita[3], Masaru Tomita[2] and Mitsuhiro Itaya[2,*]

[1]*Graduate School of Media and Governance, Keio University, 5322 Endo, Fujisawa-shi, Kanagawa, 252-8520;* [2]*Institute for Advanced Biosciences, Keio University, 403-1 Nipponkoku, Daihouji, Tsuruoka-shi, Yamagata 997-0017; and* [3]*Mitsubishi Kagaku Institute of Life Sciences, 11 Minamiooya, Machida-shi, Tokyo 194-8511, Japan*

Received September 6, 2007; accepted October 8, 2007; published online October 27, 2007

The genome of *Bacillus subtilis* 168 was modified to yield a genome vector for the cloning of DNA several Mb in size. Unlike contemporary plasmid-based vectors, this 4.2 Mb genome vector requires specific *in vivo* handling protocols because of its large size. Inversion mutagenesis, a method to modify local genome structure without gain or loss of genes, was applied intensively to the *B. subtilis* genome; this technique made possible both exchange and translocation of designated regions of the genome. This method not only reshuffles the genome of *B. subtilis*, but can provide insight into the biologic principles underlying genome plasticity.

Key words: antibiotic resistance, competence, inversion, homologous recombination, translocation, transformation.

Abbreviations: Ap, ampicillin; BGM vector, Bacillus subtilis genome vector; BS, Blasticidin S; bsr, Blasticidin S resistance gene; CHEF, contour-clamped homogeneous electric field; Em, erythromycin; erm, erythromycin resistance gene; Nm, neomycin; neo, neomycin resistance gene; Phl, phleomycin; phl, phleomycin resistance gene; Spec, spectinomycin; spc, spectinomycin resistance gene; Tc, tetracycline; tet, tetracycline resistance gene.

The genome of *Bacillus subtilis* 168 was converted to a genome vector by introduction of pBR322-based sequences used as a cloning locus (*1*, *2*). The BGM vector (standing for *Bacillus* GenoMe) has demonstrated stable accommodation of complete genomes from various sources, including *Escherichia coli* bacteriophage lambda (48.5 kb) (*1*), mitochondria from *Mus musculus* (16.5 kb) (*3*), chloroplasts from *Oryzae sativa* (135 kb) (*4*) and a 3.5 Mb genome from *Synechocystis* PCC6803 (*5*). The cloned DNA integrated in the *B. subtilis* genome stably replicates, and its sequences are conserved even through spore-formation and germination (*6*). In addition to cloning, methods for manipulating the cloned DNA in BGM have been exploited (*7*–*9*).

Because of physical shearing while in solution, DNA becomes more difficult to handle *in vitro* as it increases in size (particularly, beyond 100 kb) (*6*). Therefore, the *in vitro* engineering techniques that have become standard with plasmid vectors are of little use with the BGM system. In particular, *in vivo* protocols are needed that minimize *in vitro* manipulation of Mb-scale DNAs. In addition, alteration of the BGM vector itself, namely changing the structure of the *B. subtilis* genome, may be necessary to clone Mb-size DNA. At a practical level, cloning the *Synechocystis* genome required retaining symmetric genomic structure around the *oriC–terC* axis of the BGM vector (*5*).

Our group was the first to introduce an effective method for inducing inversion in the *B. subtilis* genome (*10*). This system supported rapid isolation of desired strains through screening for resistance to the antibiotic neomycin (Nm), which resulted after the appropriate acquisition of two incomplete neomycin resistance genes that had been inserted at the two ends of the region targeted for inversion (*10*). This method realized the alteration of the structure of a designated region without gain or loss of genes by its inversion through intrachromosomal homologous recombination. Further, the method has been applied for example, to unveil the function of a relevant genome region (polar localization region) in sporulation (*11*) and to replace long genomic region (more than several hundreds of kb), accurately without discontinuous DNA replacement (*12*). Although the utility of the altered genome structure and the significance of inversion-associated traits remained to be validated experimentally, these reports suggested that the *B. subtilis* genome structure was somewhat plastic and that inversion methods likely would be of great use for manipulating giant DNAs, both the BGM vector as well as DNAs for insertion.

In the present study, we extended our original neomycin-resistance selection method (*ne–eo* system), limited to the single 1678 kb region between *yjcI* and *ywkF*, (*10*) to other regions of the *B. subtilis* genome. Furthermore, the use of an additional antibiotic marker, tetracycline (*tet*), facilitated progressive introduction of double inversions on the *B. subtilis* genome, and we describe several resulting strains that have more complex structures than the original genome. We conclude by

*To whom correspondence should be addressed. Tel: +81 (235) 29 0526, Fax: +81 (235) 29 0530, E-mail: mita2001@sfc.keio.ac.jp

Table 1. ***Bacillus subtilis* strains used in this study.**

Strain	Relevant genotype[a]	Antibiotic markers	Construction, sources or reference[b]
168*trpC2*(=1A1)	*trpC2*		BGSC
BEST5372	[1]::*eo*−, [4]::*ne*+,	Bs^R, Spc^R	pNEXT5GA × pNEXT41FB × 168*trpC2*
BEST5122	[2]::*eo*−, [4]::*ne*+,	Bs^R, Spc^R	pNEXT38GB × pNEXT41FB × 168*trpC2*
BEST5553	[4]::*eo*+, [7]::*ne*−,	Bs^R, Spc^R	pNEXT41GB × pNEXT55FA × 168*trpC2*
BEST21434	[3]::*te*+, [8]::*et*−	Phl^R, Em^R	pBEAZ191 × pBEAZ195 × 168*trpC2*
BEST5396	[1]::*eo*+, [4]::*ne*+,	Bs^R, Spc^R	pNEXT5GB × pNEXT41FB × 168*trpC2*
BEST5129	[2]::*eo*+, [4]::*ne*+,	Bs^R, Spc^R	pNEXT38GA × pNEXT41FB × 168*trpC2*
BEST21558	[3]::*te*+, [8]::*et*+	Phl^R, Em^R	pBEAZ191 × pBEAZ194 × 168*trpC2*
BEST21441	[3]::*te*+, [8]::*et*−, [1]::*eo*+, [4]::*ne*+	Phl^R, Em^R, Spc^R, Bs^R	BEST5396 × BEST21434
BEST21481	[3]::*te*+, [8]::*et*−, [2]::*eo*+, [4]::*ne*+	Phl^R, Em^R, Spc^R, Bs^R	BEST5129 × BEST21434
BEST21586	[1]::*eo*−, [4]::*ne*+, [3]::*te*+, [8]::*et*+	Phl^R, Em^R, Spc^R, Bs^R	BEST21558 × BEST5372
BEST21569	[2]::*eo*−, [4]::*ne*+, [3]::*te*+, [8]::*et*+	Phl^R, Em^R, Spc^R, Bs^R	BEST21558 × BEST5122
BEST21488	[4]::*eo*+, [7]::*ne*−, [3]::*te*+, [8]::*et*−	Phl^R, Em^R, Spc^R, Bs^R	BEST5553 × BEST21434
BEST5227	inv[3-8]N	Nm^R, Bs^R, Spc^R	(10)
BEST5744	inv[1-4]N	Nm^R, Bs^R, Spc^R	BEST5372 → Nm
BEST5162	inv[2-4]N	Nm^R, Bs^R, Spc^R	BEST5122 → Nm
BEST5623	inv[4-7]N	Nm^R, Bs^R, Spc^R	BEST5553 → Nm
BEST21437	inv[3-8]T	Tc^R, Phl^R, Em^R	BEST21434 → Tc
BEST21465	inv[3-8]T, [1]::*eo*+, [4]::*ne*−	Tc^R, Phl^R, Em^R, Spc^R, Bs^R	BEST21441 → Tc
BEST21503	inv[3-8]T, [2]::*eo*+, [4]::*ne*−	Tc^R, Phl^R, Em^R, Spc^R, Bs^R	BEST21481 → Tc
BEST21593	inv[1-4]N, [3]::*te*−, [8]::*et*+	Nm^R, Phl^R, Em^R, Spc^R, Bs^R	BEST21586 → Nm
BEST21575	inv[2-4]N, [3]::*te*−, [8]::*et*+	Nm^R, Phl^R, Em^R, Spc^R, Bs^R	BEST21569 → Nm
BEST21474	inv[3-8]T/[1-4]N	Nm^R, Tc^R, Phl^R, Em^R, Spc^R, Bs^R	BEST21465 → Nm
BEST21524	inv[3-8]T/[2 -4]N	Nm^R, Tc^R, Phl^R, Em^R, Spc^R, Bs^R	BEST21503 → Nm
BEST21598	inv[1-4]N/[3-8]T	Nm^R, Tc^R, Phl^R, Em^R, Spc^R, Bs^R	BEST21593 → Tc
BEST21581	inv[2-4]N/[3-8]T	Nm^R, Tc^R, Phl^R, Em^R, Spc^R, Bs^R	BEST21575 → Tc

[a](+) and (−) indicate clockwise and counterclockwise orientations with respect to *oriC*, respectively, in the *B. subtilis* circular genome; numbers in square brackets are those defined in Table 2. [b]BGSC, *Bacillus subtilis* Genetic Stock Center; arrow indicates selection of inversion mutant by Nm or Tc from the parental strain.

discussing the implications of reshuffling of the *B. subtilis* genome with respect to both genome engineering and genome biology.

MATERIALS AND METHODS

Bacterial Strains and Culture Media—Escherichia coli strain DH5α (F⁻ F80d*lacZ*D*M15* D [*lacZYA-argF*] *U169 deoR recA1 endA1 hsdR17* [r_K^-, m_K^+] *phoA supE44* l⁻ *thi*-1 *gyrA96 relA1*) was used as the host for molecular cloning. *Bacillus subtilis* strains used in this study are listed in Table 1. Both bacteria were grown in Luria-Bertani broth (LB) at 37°C unless specified. Solid media was prepared by adding agar (1.5% w/v) to LB for *E. coli* or to antibiotic medium 3 (Difco, Sparks, MD, USA) for *B. subtilis*. Tetracycline (Tc, 10 μg/ml) and ampicillin (Ap, 50 μg/ml) were added for DH5α selection. Blasticidin S (BS, 250 μg/ml), erythromycin (Em, 5 μg/ml), neomycin (Nm, 3 μg/ml), spectinomycin (Spec, 50 μg/ml), phleomycin (Phl, 1.5 μg/ml) and Tc (10 μg/ml) were added for *B. subtilis* selection. Strains were tested for containing multiple antibiotic resistance genes by using a replica plating method. Preparation and transformation of competent *E. coli* and *B. subtilis* cells were done as previously described (*13*).

DNA Isolation and Manipulation—Plasmid DNA was isolated from *E. coli* transformants by QIAprep Spin Miniprep Kit (Qiagen, Valencia, CA, USA). *Bacillus subtilis* genomic DNA was extracted by liquid isolation method (*14*) and used for transformation. Intact unsheared *B. subtilis* genomic DNA for contour-clamped homogeneous electric field (CHEF) electrophoresis was prepared in agarose gel plugs, as described elsewhere (*13*). I-*Sce*I was purchased from Roche (Mannheim, Germany), I-*Ppo*I from Promega (Madison, WI, USA), *Sfi*I and I-*Ceu*I from New England Biolabs (Ipswich, MA, USA) and other restriction endonucleases from Toyobo (Kyoto, Japan). The DNA ligation kit was purchased from Takara (Shiga, Japan). Primers were synthesized by Nihon Gene Research Laboratories (Miyagi, Japan).

Electrophoresis and Southern Hybridization—CHEF gel electrophoresis was conducted using agarose gels (1.0% w/v) in TBE solution (50 mM Tris–borate [pH 8.0], 1.0 mM EDTA) with running conditions as described in the legend to Fig. 2B. Agarose gels (1.0% w/v) in TAE solution (50 mM Tris–acetate [pH 8.0], 1.0 mM EDTA) were used for conventional gel electrophoresis at room temperature. After electrophoresis, gels were stained in ethidium bromide solution and visualized under UV light.

A non-radioactive labelling nucleotide, digoxigenin-11-dUTP, was used for Southern hybridization. Probes were prepared by using the PCR DIG probe synthesis kit (Roche, Mannheim, Germany) with specific primers. Labelled bands were detected with DIG Nucleic Acid Detection Kit (Roche) followed by 5-Bromo-4-Chloro-3′-Indolylphosphatase p-Toluidine salt and nitro-blue tetrazolium chloride (Sigma-Aldrich, St Louis, MO, USA).

Construction of ne *and* eo *Cassettes for Induction of Inversion*—The effectiveness of the *ne–eo* system was

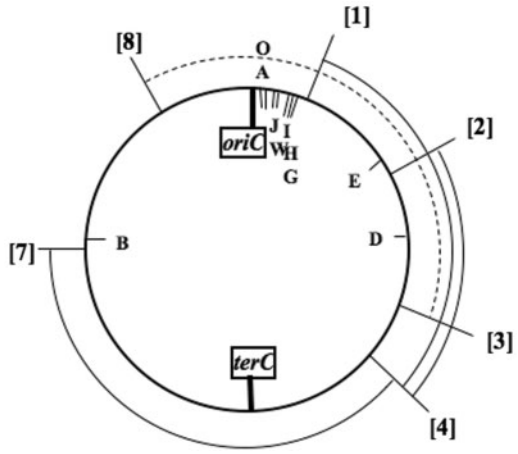

Fig. 1. **Inverted regions of the *B. subtilis* 168 genome.** *Bacillus subtilis* genome is represented as a circle, with the locations of *oriC*, *terC* and 10 ribosomal RNA operons (*rrnO, A, J, W, I, H, G, E, D* and *B*) indicated. All endpoints of inversions examined in the present study are the same *Not*I recognition sites adopted in the previous report (*15*). Nucleotide sequence number, names of the gene and gene function of each locus number shown in parenthesis are as follows, respectively. Locus [1]: 178,413, in *ybaR*, unknown; [2]: 752,533, between *yeeI* and *yeeK*; [3]: 1,258,347, in *yjcI*, unknown; [4]: 1,553,998, in *pycA*, pyruvate carboxylase; [7]: 3,120,299, in *ytqB*, unknown; [8]: 3,794,952, in *ywkF*, unknown. Solid lines indicate segments inverted by using the *ne–eo* system in the present study. Dotted lines indicate segments inverted previously by using the *ne–eo* system (*10*) and by using the *te–et* system in this study.

evaluated further by applying this method to three additional genomic regions (Fig. 1). Endpoints of these inversions are the *Not*I recognition sites of the *B. subtilis* genome, numbered as in the previous report (*15*). These sites are in the genes *ybaR*: [1], *yeeIK*: [2], *yjcI*: [3], *pycA*: [4], *ytqB*: [7], and *thrZ*: [8] (Fig. 1). These *Not*I recognition sites were included in the *Not*I-linking clones in the pNEXT-series plasmid used for construction of the physical map (*13*) and are dispensable for growth even after simultaneous mutagenesis of these sites (*16*). The *ne* and *eo* cassettes isolated by *Not*I digestion of pBEST518 and pBEST524B (*10*) were ligated into the *Not*I site of the original pNEXT plasmids. The resultant plasmids prepared in *E. coli*—pNEXT5GA at [1], pNEXT38GB at [2], pNEXT41FB at [4], pNEXT41GB at [4], and pNEXT55FA at [7]—are listed in Table 2. These were used to insert the *ne* or *eo* cassette into the respective *Not*I loci of the *B. subtilis* genome. The constructed plasmids were linearized with the restriction enzymes listed in Table 2 on transformation of *B. subtilis* to yield BEST5372, 5122 and 5553 (Table 1). Integrants were selected by use of antibiotic markers, *spc* for the *ne* cassette and *bsr* for the *eo* cassette (*10*).

Construction of te *and* et *Cassettes for Induction of Inversion Selectable by Tc*—Two incomplete *tet* genes sharing a 1095 bp overlapped region were constructed as the molecular apparatus designated as the *te–et* system. The fragment corresponding to the *te* fragment (1530 bp) was PCR amplified from pBEST307 (*17*) by using the primer set te-F (TAATCTAGACCATATTGTGTATA AGTGATGAA) and te-R (ATCTGCAGCTAATGACAAT GATTCCTGAAA) and cloned into pUC18. The Em resistance gene (*erm*) isolated from pBEST703 (*18*) was inserted downstream of the *te* fragment and subsequently modified by using PCR amplification to add *Not*I sites at both ends. The amplified 3.0 kb *te* cassette was cloned into pBR322, resulting in pBEST10010 from which the *te* cassette was prepared after *Not*I digestion. Two I-*Ppo*I recognition sites were created just inside the two *Not*I sites by insertion of appropriate linkers.

The fragment corresponding to the *et* cassette, the 1208 bp *et* fragment linked to a Phl resistance gene (*phl*), was constructed similarly. The *et* fragment and *phl* gene were PCR amplified from pBEST43ETP (kindly donated by M. Ogura, Tokai University, Kanagawa, Japan) by using the primers etup-phlup2 (CCGTTAATGCGC CATTCAAAAGGTTACTCC), etdn (AAAGCGGCCGCGA ATTCCTGTTATAAAAAAAGGATC), phldn (TTTGCGGC CGCTGATTTCACTTTTTGCATTCTAC), and phlup-etup2 (TTATAACAGGAATTCATGGCGCATTAACGG), and the resulting products were combined by using the splicing by overlap extension (SOE)-PCR method (*19*) with the primers etdn and phldn. The amplified 2.2 kb *et* cassette was cloned into pHASH202 (kindly donated by Y. Ohashi, Human Metabolome Technologys, Yamagata, Japan), resulted in pBEAZ150. The *Not*I-linking clones of loci 3 and 8, pBEAZ179 and pBEAZ192 (Table 2) were newly prepared by PCR and cloned into pCR2.1 (see footnote to Table 1). The *te* cassette in pBEST10010 was isolated and cloned into the *Not*I site of pBEAZ179, resulting in pBEAZ191, which was used to insert the *te* cassette into locus 3. Similarly, the *et* cassette isolated from pBEAZ150 was ligated into the *Not*I site of pBEAZ192, resulting in pBEAZ195, which was used to insert the *et* cassette into locus 8. The pBEAZ191 and pBEAZ195 were linearized with *Bgl*II prior to transformation of *B. subtilis*. Transformants were selected for resistance to Em (for pBEAZ191) and Phl (for pBEAZ195) (Table 1).

Isolation of Inversion Mutants Created by the ne–eo *and* te–et *Systems*—The procedure for isolating inversion mutants as colonies was described in the previous report (*10*). Briefly, the strains harbouring the two cassettes were cultured in LB medium at 37°C until stationary phase. During cell division, intrachromosomal homologous recombination within the internal homologous region, 590 bp for *ne–eo* or 1095 bp for *te–et*, forms functional *neo* or *tet* gene after inversion of the flanking genomic region (Fig. 2A). The single inversion was selected as colonies on solid media containing Nm or Tc; selection for the second inversion was done similarly. With successful inversion, the two I-*Sce*I sites originally located within the *ne* cassette are separated to the two endpoints of inversion, giving rise to a I-*Sce*I fragment that is equivalent in size to the inverted region ((*10*) and Fig. 2A). Similarly, the two I-*Ppo*I sites originally located within the *te* cassette (Fig. 2A) should be relocated to the two endpoints of inversion, giving rise to a I-*Ppo*I fragment equivalent in size to the inverted region. The inversion efficiency was calculated as described (*10*).

Experimental Criteria for the Inversion Mutant—The structure of the *B. subtilis* inversion mutant should meet the following five criteria: (i) yield I-*Ppo*I or I-*Sce*I

Table 2. **Plasmids used in this study.**

Plasmid	Insert[a]	Abbreviation	Antibiotics makers	Enzyme to linearize	Source or references
pBR322			Ap^R		
pCR2.1			Ap^R		Invitrogen
pHASH202[b]			Ap^R		Y. Ohashi
pBEST518	*ne*		Ap^R, Spc^R		(13)
pBEST524B	*eo*		Ap^R, Bs^R		(13)
pBEST307	*tet*		Tc^R		(17)
pBEST703	*erm*		Em^R		(18)
pBEST43ETP	*phl*		Phl^R		M. Ogura
pBEST10010	*te*		Ap^R, Em^R		This study
pBEAZ150	*et*		Ap^R, Phl^R		This study
pNEXT5	*ybaR*	[1]	Tc^R, Em^R		(13)
pNEXT38	*yeeIK*	[2]	Ap^R, Tet		(13)
pBEAZ179[c]	*yjcI*	[3]	Ap^R		This study
pNEXT41	*pycA*	[4]	Ap^R, Tc^R		(13)
pNEXT55	*ytqB*	[7]	Ap^R		(13)
pBEAZ192[d]	*ywkF*	[8]	Ap^R		This study
pNEXT5GA	*ybaR*::*eo*−	[1]::*eo*−	Bs^R, Tc^R, Em^R	EcoRV	This study
pNEXT5GB	*ybaR*::*eo*+	[1]::*eo*+	Bs^R, Tc^R, Em^R	EcoRV	This study
pNEXT38GA	*yeeIK*::*eo*+	[2]::*eo*+	Ap^R, Bs^R, Tc^R	SalI	This study
pNEXT38GB	*yeeIK*::*eo*−	[2]::*eo*−	Ap^R, Bs^R, Tc^R	SalI	This study
pBEAZ191	*yjcI*::*te*+	[3]::*te*+	Ap^R, Em^R	BglII	This study
pNEXT41FB	*pycA*::*ne*+	[4]::*ne*+	Ap^R, Spc^R, Tc^R	PvuII	This study
pNEXT41GB	*pycA*::*eo*+	[4]::*eo*+	Ap^R, Bs^R, Tc^R	SalI	This study
pNEXT55FA	*ytqB*::*ne*−	[7]::*ne*−	Ap^R, Spc^R	BamHI	This study
pBEAZ194	*ywkF*::*et*+	[8]::*et*+	Ap^R, Phl^R	BglII	This study
pBEAZ195	*ywkF*::*et*−	[8]::*et*−	Ap^R, Phl^R	BglII	This study

[a](+) and (−) indicate clockwise and counterclockwise orientations, respectively, in the *B. subtilis* circular genome, respectively. [b]pHASH202 was derived from pHASH102 (*35*) by adding *Pma*CI, *Pvu*II and I-*Ppo*I recognition sites. [c]*Not*I-linking clone prepared by PCR amplification of the 2012-bp fragment (nucleotides 1 257 359–1 259 370) from the *B. subtilis* genome. [d]*Not*I-linking clone prepared by PCR amplification of the 2025-bp fragment (nucleotides 3 793 952–3 795 976) from the *B. subtilis* genome.

fragments that are resolvable by CHEF gel electrophoresis; (ii) give rise to 10 I-*Ceu*I fragments, which are produced by I-*Ceu*I recognition sites residing in the 16S RNA gene of the 10 *rrn* ribosomal DNA operons (Fig. 1), resolvable by CHEF gel electrophoresis (*20*); (iii) produce *Not*I fragments that are resolvable by CHEF electrophoresis (data not shown); (iv) produce *Sfi*I fragments that are resolvable by CHEF electrophoresis and that hybridize with *neo* or *tet* probe (data not shown) and (v) change the local structure of the inversion endpoints through intrachromosomal homologous recombination. Because homologous recombination is restricted within the cassettes, the expected change in the size of the corresponding *Not*I fragments highlights the inversion. The *ne* (2.4 kb) and the *eo* (1.4 kb) cassettes were converted to *neo* (1.3 kb) and *e* (2.5 kb); similarly *te* (3.0 kb) and *et* (2.2 kb) gave rise to *tet* (1.6 kb) and *e* (3.6 kb). These changes were detected by Southern hybridization of *Not*I digests by using the *neo* or *tet* gene as probe (Fig. 2B).

RESULTS

Three Single-inversion Mutants Constructed by ne–eo *system—Bacillus subtilis* 168 genome possesses symmetry in length around the *oriC–terC* axis (*21*, *22*). In the first, *B. subtilis* inversion mutant isolated by using the *ne–eo* system, endpoints 3 and 8 were located on both replichores (Fig. 1). The genotype of the inversion mutant is defined as inv[3-8]N, indicating an inversion mutation between loci 3 and 8 and selectable by Nm (Table 1). Successful inversion of the 1678 kb region altered the lengths of these two replichores (Fig. 2A). In addition, we assessed the effectiveness of the *ne–eo* system for three additional regions. Parental strains BEST5372 ([1]-[4]), BEST5122 ([2]-[4]), and BEST5553 ([4]-[7]) all contained the *ne* and *eo* cassettes integrated in head-to-head orientation at the indicated loci and were sensitive to Nm. The endpoints of inversions [1-4] (801 kb) and [2-4] (1376 kb) are within the same replichore, but [4-7] (1566 kb) is between two replichores (Fig. 1). The viable inversion mutants BEST5744 (inv [1-4]N), BEST5162 (inv[2-4]N), and BEST5623 (inv [4-7]N) were obtained on plates containing Nm and incubated at 37°C. The inverted regions for these strains were validated by restriction digestion with I-*Sce*I, I-*Ceu*I *Not*I and *Sfi*I analyses [data not shown, but similar to CHEF data (*10*)]. Formation of an intact *neo* gene and its complementary *e* segment at the inversion junctions (similar to those indicated in Fig. 2A) was confirmed by Southern analysis using the *neo* gene as a probe (data not shown). BEST5744 (inv[1-4]N) formed significantly smaller colonies than the parental strain, BEST5372, on LB plate at 37°C (Fig. 3). BEST5744 (inv[1-4]N) likely is manifesting the adverse effects of multiple inversely oriented genes within the inverted region; this arrangement perhaps increases the frequency of collision between transcription and replication machineries (*23*).

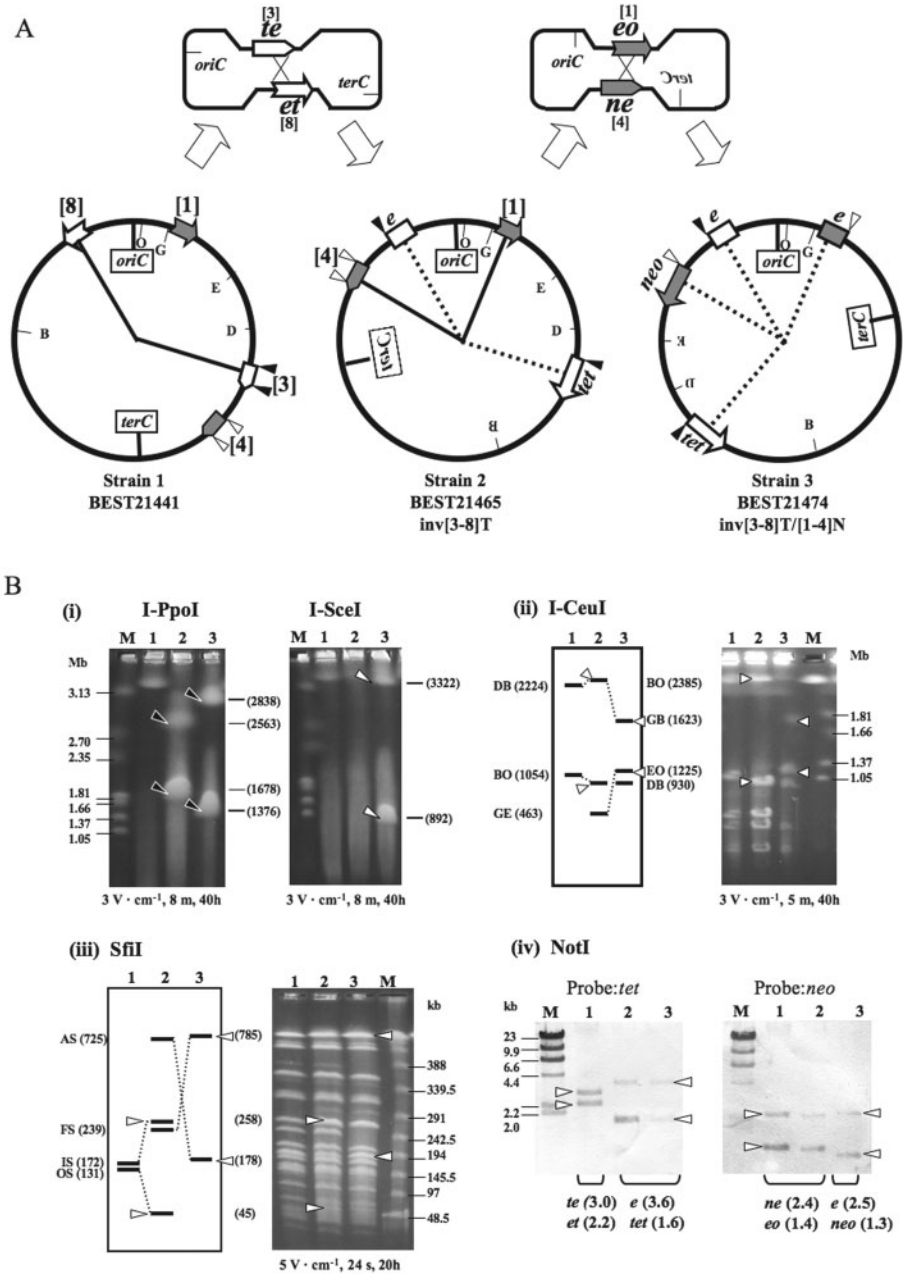

Fig. 2. **A strain acquired double inversions using *ne–eo* and *te–et* system.** (A) A circular *B. subtilis* genome carrying the four cassettes in strain 1 (BEST21441) is shown at the left. The intrachromosomal homologous recombination between the cassettes *te* and *et* (top left) resulted in strain 2 (BEST21465), which has a single inversion (on the middle). Subsequent intrachromosomal homologous recombination between the cassettes *ne* and *eo* (top right) caused the additional inversion mutation in strain 3 (BEST21474) on the right. In strain 2, the two I-*Ppo*I sites (open arrowheads) originally within the *te* cassette at locus [3] of strain 1 are separated and now reside at [3] and [8]. This relocation yielded the two I-*Ppo*I fragments presented in (B). Similarly, the two I-*Sce*I sites (closed arrowheads) within locus [4] of the *eo* cassette were separated to sites [1] and [4], giving rise to the two large I-*Sce*I fragments of strain 3 (B). The sizes of the I-*Ppo*I fragments of strain 2 varied according to the additional inversion. Only the locations of relevant *rrn* operons, equivalent to the I-*Ceu*I sites, are indicated inside the circular genome. First, only inversions supporting *tet* selection occur, due to the designed orientation of the *ne* and *eo* cassettes (see text). (B) Changes in sizes of relevant fragments according to correct inversion mutation. Lanes are labelled with the strain numbers, as defined (A). (i) I-*Ppo*I and I-*Sce*I fragments obtained from the indicated strains. The arrowheads indicating the fragments are the same as described in (A). The calculated sizes of the fragments are indicated to the right and are comparable with the *Hansenula wingei* chromosomal makers run in lane M, the sizes of which are indicated to the left of the photos. (ii) I-*Ceu*I fragments resolved by CHEF (right panel); relevant fragments are drawn schematically in the left panel. *H. wingei* chromosomal marker was run in lane M. (iii) *Sfi*I fragments resolved by CHEF (right panel); relevant fragments are drawn schematically in the left panel. All 26 *Sfi*I fragments (AS–ZS) were named in reference (*13*). Concatemeric lambda DNA marker (48.5 kb × *n*) was run in lane M, with the sizes of the fragments listed on the right. (iv) Alteration in sizes of cassettes due to intrachromosomal homologous recombination. Calculated cassette size was provided by *Not*I fragments identified through Southern hybridization using the indicated probes. Lambda/*Hin*dIII fragments were run in lane M.

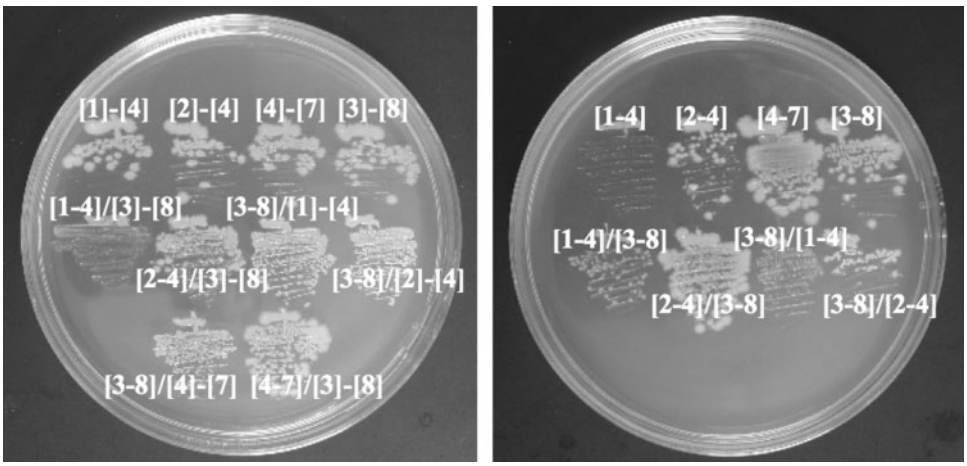

Fig. 3. **Growth of parental and inverted strains on LB plates**. Parental strains (left panel) and inverted strains (right panel) were incubated at 37°C for 17 and 24 h, respectively. Genotypes of each strain are indicated: [1]-[4], [2]-[4], [4]-[7] and [3]-[8] are parental strains of corresponding single inversions [1-4], [2-4], [4-7] and [3-8], respectively. [1-4]/[3]-[8], [2-4]/[3]-[8], [3-8]/[1]-[4], [3-8]/[2]-[4], [3-8]/[4]-[7] and [4]-[7]/[3-8] are parental strains of corresponding double inversions harbouring single inversions.

A Single-inversion Mutant Constructed by te–et *System*—Given these viable single inversion mutants, we endeavoured to introduce additional inversion mutations. First, to reuse the *ne–eo* system, we removed the *neo* and *e* fragments at the inversion endpoints of BEST5227 (*10*) by using gene-directed mutagenesis (*24*). From the Nm-sensitive inv[3-8] mutant, we obtained double-inversion mutants similar to those described in the next section (data not shown). However, removal of absolutely every sequence of the antibiotic resistance genes was time-consuming and not applicable for strains that unexpectedly lost competency. We therefore constructed another inversion induction apparatus by using a *tet* gene for rapid selection of double-inversion mutants. The *te* and *et* cassettes were inserted in loci 3 and 8, monitored by using the linked antibiotic resistance markers *erm* and *phl* and resulted in the parental strain BEST21434 (Table 1). Similar to the inv[3-8]N strain, inv[3-8]T mutant represented by BEST21437 was isolated as a strain resistant to Tc. The estimated frequency of inversion according to Tc resistance, $1.0 \pm 0.8 \times 10^{-6}$/cell generation, was more than 10 times to that previously obtained through selection with Nm ($6.9 \pm 1.4 \times 10^{-8}$/cell generation). This enhancement is consistent with the nearly doubled length of the region for intrachromosomal homologous recombination (Fig. 2A): 1095 bp for *te–et* compared with 590 bp of *ne–eo*.

Isolation of Strains Acquiring Double Inversion—With the availability of two inversion systems, we expected to generate double-inversion mutants through consecutive induction of inversion. Appropriate orientation (that is, head-to-head) of the *ne* and *eo* (or *te* and *et*) in the genome likely is vitally important; therefore, if one of the endpoints of the second inversion is located within the region altered in the first inversion, the orientation of the cassette should be reversed from the beginning. For double mutants arising from inv[3-8]T followed by inv[1-4]N or inv[2-4]N, the *eo* cassette at locus 1 or 2 was reversed compared with that of the parent for the single-inversion mutant. The case of inv[3-8]T/[1-4]N (the genotype of the double-inversion mutant is defined as such) is drawn in Fig. 2A, in which the two sets of inversion apparatus are integrated in parental strain BEST21441. Antibiotic selection by Tc (BEST21465) followed by Nm gave rise to the double mutant BEST21474. This strain formed small colonies (Fig. 3). Similarly, the double-inversion mutant BEST21524 (inv[3-8]T/[2-4]N) was obtained by starting with BEST21481 and shuttling through BEST21503 (Table 1). The genomic structure of the inversion mutants was confirmed by restriction digestion with I-*Ppo*I, I-*Sce*I, I-*Ceu*I, *Not*I and *Sfi*I, followed by CHEF electrophoresis (Fig. 2B).

Different Strains Acquiring the Double Inversion in Different Order—Depending on the order of acquisition, the two possible inversion patterns of regions [3]-[8] and [1]-[4] yield strains with different genomic structures. The parental strain BEST21586, in which *ne* and *eo* were integrated at [4] and [1] in head-to-head orientation, contained the *te* cassette at [3] in reverse orientation. The double-inversion mutant BEST21598 (inv[1-4]N/[3-8]T) was obtained by manipulating Nm-resistant BEST21593 (inv[1-4]N). Similarly, BEST21581(inv[2-4]N/[3-8]T) was isolated by starting from BEST21569 and shuttling through Nm-resistant BEST21575 (inv[2-4]N). The genomic structures were verified by restriction digestion with I-*Ppo*I, I-*Sce*I, I-*Ceu*I, *Not*I and, *Sfi*I, and Southern hybridization confirmed the correct double inversion (data not shown). The regions and orientations of the inverted regions of mutants constructed in this study are presented in Fig. 4. The different patchwork structures clearly vary according to the order of acquisition, as mentioned in the legend to Fig. 4.

Double Parallel Inversion Mutant—We also attempted sequential inversion of two regions that do not overlap, designated as parallel inversion. In the present study, only two such mutants (inv[3-8]T/[4-7]N and inv[4-7]N/[3-8]T) were possible. Unlike the double-inversion mutant described in the previous section, those generated through parallel inversion had no need for reversion

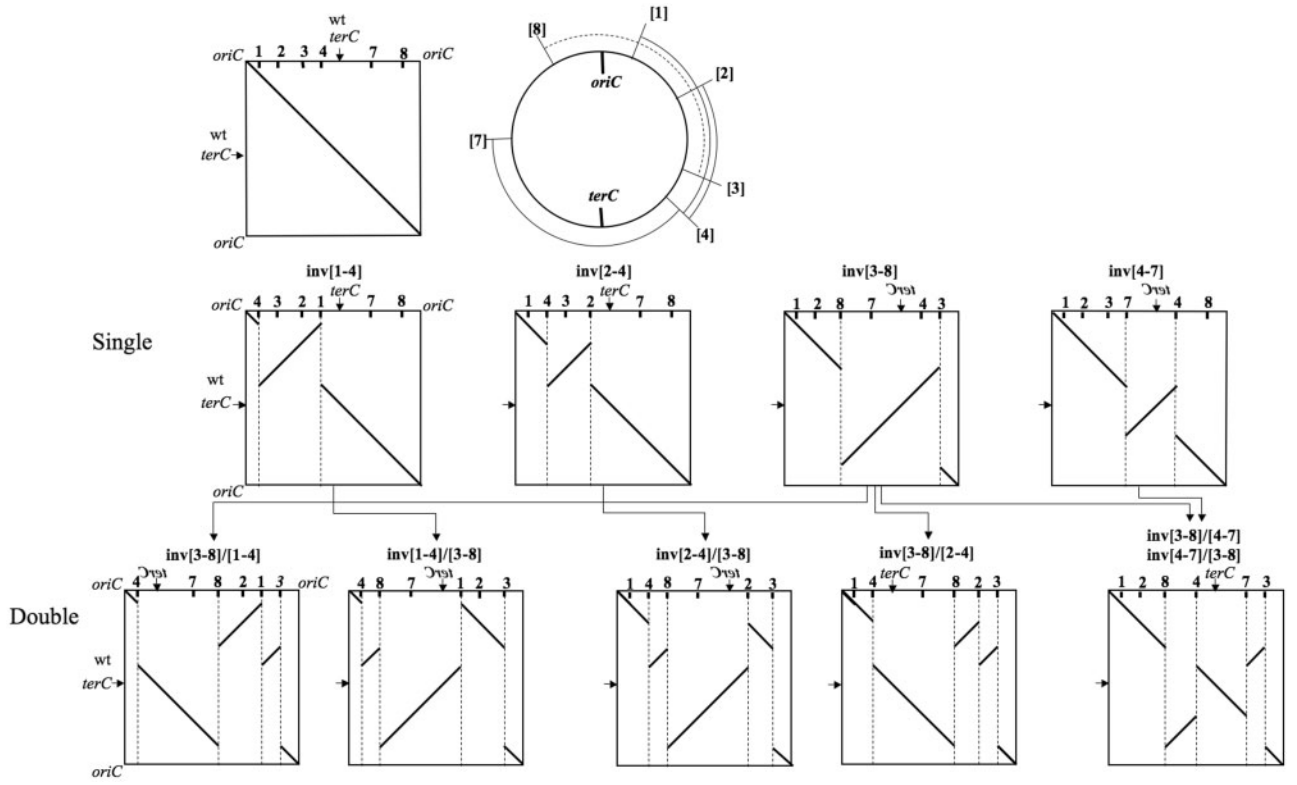

Fig. 4. **View of genome structure linearized at *oriC* locus**. The vertical axis represents the genome of wild-type (wt) *B. subtilis* 168, and the horizontal axis represents the genomes of the inversion mutants indicated. The positions of the genes in the inversion mutants relative to that of the wt strain are drawn. The dashed horizontal lines inside the box indicate the inversion endpoints, with their locations at the top. At the bottom, the different genomic structures possible depending on the order and region of the two inversion mutations are emphasized. As the location of *terC* is away from the centre of horizontal axis, the genomic asymmetry becomes higher.

of one of the inserted cassettes, and these two mutants should have the same genomic structure (Fig. 4). The parental strain BEST21488 first generated inversion mutant BEST21511 (selected by Nm) or BEST21513 (selected by Tc). Curiously, the number of colonies selected after the second inversion was reduced by more than 100-fold for both routes (data not shown). We isolated two strains that met the four of five criteria regarding genomic structure (described in MATERIALS AND METHODS section); some deletions were found in both strains outside the target region by *Not*I digestion and CHEF electrophoresis (failure to meet the third criteria). Therefore, we left out both strains from candidates. Because the parental single-inversion mutants were recombination-proficient and the antibiotic resistance gene was regenerated correctly, the dramatic reduction of the number of colony formation might be caused by the structural constraints of the genome of the double parallel inversion strains. The additional parallel double-inversion mutants we have planned will help answer this question.

DISCUSSION

The structure of the 4215 kb *B. subtilis* genome can be modified by (i) insertion of DNA from various non-cognate sources (*1–3*, *5*, *6*, *16*, *25*), (ii) replacement with DNA from genetically related strains (*15*, *26*, *27*), (iii) multiplication (*28–30*) and (iv) deletion of dormant lysogenic phages, and systematic inactivation of non-essential genes (*31*, *32*). These insertions and deletions of DNA segments into or from the *B. subtilis* genome increase or decrease the size of the genome and add or remove genes that can affect gene networks and genetic traits. In contrast, intrachromosomal rearrangement such as inversion does not alter gene content. Furthermore, inversion steps composed of homologous recombination and the subsequent DNA replication proceed all in *in vivo* environment. This genetic technique limits the manipulation of fragile giant DNAs in solution. Therefore, inversion mutagenesis is suited to genome-scale manipulation, an urgent need unveiled during the construction of a *B. subtilis*-based chimeric genome (*5*).

We extended the application of a prototype procedure to induce inversion mutation in wild-type *B. subtilis* 168 (*10*) to additional regions of the *B. subtilis* genome and obtained several viable inversion mutants. Both regions whose endpoints both were located within a single replichore and on opposite sides of the *oriC–terC* axis could be inverted. These results encouraged us not only to modify DNA fragments cloned into the BGM vector but also to further adapt the *B. subtilis* 168 genome for various aims. For example, two *B. subtilis* operons

located in different replichores are being juxtaposed and assembled by inversion mutation (R. Uotsu *et al*., unpublished data). Furthermore, using a *te–et* apparatus in addition to *ne–eo* successfully yielded more complicated genome structures (Fig. 4). The two systems we have designed likely will facilitate rearrangement of giant (Mb-range) DNA constructs. In particular, this method could be applied to assemble the *Synechocystis* PCC 6893 genome DNA fragments currently cloned as three independent inserts into a single segment in BGM vector (*5*).

The inversion mutants isolated in the present study varied slightly in their growth rates. Regarding the biological significance of inversion mutagenesis, the apparent changes induced by inversion mutagenesis can be allocated into two categories. In one category, the orientation of genes in the inverted region is reversed with respect to *oriC* if the inversion takes place in a single replichore. Given the bias of gene orientation in the genome, 75% of genes are located on the leading strand (*33*); reverse orientation of a large proportion of these genes could affect their expression and hamper growth of *B. subtilis*. The inv[1-4], which exhibited significantly slow growth, is classified into this category. In the other category, the lengths of two replichores divided by the *oriC–terC* axis altered if the inversion takes place around the axis. The genomic symmetry around the *oriC–terC* axis is important for optimal cell growth, and naturally isolated inversion strains of diverse genera show symmetrical genomic structure (*34*). The inv[3-8]/[1-4], which exhibited significantly slow growth, is classified into this category. Though inv[3-8]/[4-7] and inv[4-7]/[3-8] are classified into neither categories, these strains harbouring expected genome structures were not obtained. This result implies that complete double parallel inversions might be lethal due to some unknown constraints of their genome structures. We currently are creating additional viable inversion mutants that cover the entire *B. subtilis* genome region to facilitate a comprehensive, qualitative comparison of their biological traits.

We thank to Drs K. Tsuge (Keio University, Yamagata, Japan) and Y. Naito (Keio University, Kanagawa, Japan) for useful discussions. This work was supported by Grant-in-Aid for the 21st Century Center of Excellence (COE) Program, entitled "Understanding and Control of Life's Function via Systems Biology" (to Keio University, Japan).

REFERENCES

1. Itaya, M. (1995) Toward a bacterial genome technology: integration of the *Escherichia coli* prophage lambda genome into the *Bacillus subtilis* 168 chromosome. *Mol. Gen. Genet.* **248**, 9–16
2. Itaya, M., Nagata, T., Shiroishi, T., Fujita, K., and Tsuge, K. (2000) Efficient cloning and engineering of giant DNAs in a novel *Bacillus subtilis* genome vector. *J. Biochem.* **128**, 869–875
3. Yonemura, I., Nakada, K., Sato, A., Hayashi, J., Fujita, K., Kaneko, S., and Itaya, M. (2007) Direct cloning of full-length mouse mitochondrial DNA using a *Bacillus subtilis* genome vector. *Gene* **391**, 171–177
4. Itaya, M., Fujita, K., Kuroki, A., and Tsuge, K. Bottom-up genome assembly using the *Bacillus subtilis* genome vector. *Nature Methods*, in press
5. Itaya, M., Tsuge, K., Koizumi, M., and Fujita, K. (2005) Combining two genomes in one cell: stable cloning of the *Synechocystis* PCC6803 genome in the *Bacillus subtilis* 168 genome. *Proc. Natl Acad. Sci. USA* **102**, 15971–15976
6. Kaneko, S., Akioka, M., Tsuge, K., and Itaya, M. (2005) DNA shuttling between plasmid vectors and a genome vector: systematic conversion and preservation of DNA libraries using the *Bacillus subtilis* genome (BGM) vector. *J. Mol. Biol.* **349**, 1036–1044
7. Tsuge, K. and Itaya, M. (2001) Recombinational transfer of 100-kilobase genomic DNA to plasmid in *Bacillus subtilis* 168. *J. Bacteriol.* **183**, 5453–5458
8. Tomita, S., Tsuge, K., Kikuchi, Y., and Itaya, M. (2004) Targeted isolation of a designated region of the *Bacillus subtilis* genome by recombinational transfer. *Appl. Environ. Microbiol.* **70**, 2508–2513
9. Kuroki, A., Ohtani, N., Tsuge, K., Tomita, M., and Itaya, M. (2007) Conjugational transfer system to shuttle giant DNA cloned by *Bacillus subtilis* genome (BGM) vector. *Gene* **399**, 72–80
10. Toda, T., Tanaka, T., and Itaya, M. (1996) A method to invert DNA segments of the *Bacillus subtilis* 168 genome by recombination between two homologous sequences. *Biosci. Biotechnol. Biochem.* **60**, 773–778
11. Wu, L.J. and Errington, J. (2002) A large dispersed chromosomal region required for chromosome segregation in sporulating cells of *Bacillus subtilis*. *EMBO J.* **21**, 4001–4011
12. Liu, S., Endo, K., Ara, K., Ozaki, K., and Ogasawara, N. (2007) The accurate replacement of long genome region more than several hundreds kilobases in *Bacillus subtilis*. *Genes Genet. Syst.* **82**, 9–19
13. Itaya, M. and Tanaka, T. (1991) Complete physical map of the *Bacillus subtilis* 168 chromosome constructed by a gene-directed mutagenesis method. *J. Mol. Biol.* **220**, 631–648
14. Saito, H. and Miura, K.I. (1963) Preparation of transforming deoxyribonucleic acid by phenol treatment. *Biochim. Biophys. Acta* **72**, 619–629
15. Itaya, M. (1997) Physical map of the *Bacillus subtilis* 166 genome: evidence for the inversion of an approximately 1900-kb continuous DNA segment, the translocation of an approximately 100-kb segment and the duplication of a 5-kb segment. *Microbiology* **143(Pt 12),**3723–3732
16. Kobayashi, K., Ehrlich, S.D., Albertini, A., Amati, G., Andersen, K.K., Arnaud, M., Asai, K., Ashikaga, S., Aymerich, S., Bessieres, P., Boland, F., Brignell, S.C., Bron, S., Bunai, K., Chapuis, J., Christiansen, L.C., Danchin, A., Debarbouille, M., Dervyn, E., Deuerling, E., Devine, K., Devine, S.K., Dreesen, O., Errington, J., Fillinger, S., Foster, S.J., Fujita, Y., Galizzi, A., Gardan, R., Eschevins, C., Fukushima, T., Haga, K., Harwood, C.R., Hecker, M., Hosoya, D., Hullo, M.F., Kakeshita, H., Karamata, D., Kasahara, Y., Kawamura, F., Koga, K., Koski, P., Kuwana, R., Imamura, D., Ishimaru, M., Ishikawa, S., Ishio, I., Le Coq, D., Masson, A., Mauel, C., Meima, R., Mellado, R.P., Moir, A., Moriya, S., Nagakawa, E., Nanamiya, H., Nakai, S., Nygaard, P., Ogura, M., Ohanan, T., O'Reilly, M., O'Rourke, M., Pragai, Z., Pooley, H.M., Rapoport, G., Rawlins, J.P., Rivas, L.A., Rivolta, C., Sadaie, A., Sadaie, Y., Sarvas, M., Sato, T., Saxild, H.H., Scanlan, E., Schumann, W., Seegers, J.F., Sekiguchi, J., Sekowska, A., Seror, S.J., Simon, M., Stragier, P., Studer, R., Takamatsu, H., Tanaka, T., Takeuchi, M., Thomaides, H.B., Vagner, V., van Dijl, J.M., Watabe, K., Wipat, A., Yamamoto, H., Yamamoto, M., Yamamoto, Y., Yamane, K., Yata, K., Yoshida, K., Yoshikawa, H., Zuber, U., and Ogasawara, N. (2003) Essential *Bacillus subtilis* genes. *Proc. Natl Acad. Sci. USA* **100**, 4678–4683

17. Itaya, M. (1992) Construction of a novel tetracycline resistance gene cassette useful as a marker on the *Bacillus subtilis* chromosome. *Biosci. Biotechnol. Biochem.* **56**, 685–686
18. Itaya, M., Laffan, J.J., and Sueoka, N. (1992) Physical distance between the site of type II DNA binding to the membrane and *oriC* on the *Bacillus subtilis* 168 chromosome. *J. Bacteriol.* **174**, 5466–5470
19. Horton, R.M., Hunt, H.D., Ho, S.N., Pullen, J.K., and Pease, L.R. (1989) Engineering hybrid genes without the use of restriction enzymes: gene splicing by overlap extension. *Gene* **77**, 61–68
20. Toda, T. and Itaya, M. (1995) I-*Ceu*I recognition sites in the *rrn* operons of the *Bacillus subtilis* 168 chromosome: inherent landmarks for genome analysis. *Microbiology* **141**, 1937–1945
21. Itaya, M. (1993) Integration of repeated sequences (pBR322) in the *Bacillus subtilis* 168 chromosome without affecting the genome structure. *Mol. Gen. Genet.* **241**, 287–297
22. Kunst, F., Ogasawara, N., Moszer, I., Albertini, A.M., Alloni, G., Azevedo, V., Bertero, M.G., Bessieres, P., Bolotin, A., Borchert, S., Borriss, R., Boursier, L., Brans, A., Braun, M., Brignell, S.C., Bron, S., Brouillet, S., Bruschi, C.V., Caldwell, B., Capuano, V., Carter, N.M., Choi, S.K., Codani, J.J., Connerton, I.F., and Danchin, A. (1997) The complete genome sequence of the gram-positive bacterium *Bacillus subtilis*. *Nature* **390**, 249–256
23. Wang, J.D., Berkmen, M.B., and Grossman, A.D. (2007) Genome-wide coorientation of replication and transcription reduces adverse effects on replication in *Bacillus subtilis*. *Proc. Natl Acad. Sci. USA* **104**, 5608–5613
24. Itaya, M. and Tanaka, T. (1990) Gene-directed mutagenesis on the chromosome of *Bacillus subtilis* 168. *Mol. Gen. Genet.* **223**, 268–272
25. Kaneko, S., Tsuge, K., Takeuchi, T., and Itaya, M. (2003) Conversion of sub-megasized DNA to desired structures using a novel *Bacillus subtilis* genome vector. *Nucleic Acids Res.* **31**, e112
26. Saito, Y., Taguchi, H., and Akamatsu, T. (2006) DNA taken into *Bacillus subtilis* competent cells by lysed-protoplast transformation is not ssDNA but dsDNA. *J. Biosci. Bioeng.* **101**, 334–339
27. Itaya, M. and Matsui, K. (1999) Conversion of *Bacillus subtilis* 168: *Natto* producing *Bacillus subtilis* with mosaic genomes. *Biosci. Biotechnol. Biochem.* **63**, 2034–2037
28. Mori, M., Tanimoto, A., Yoda, K., Harada, S., Koyama, N., Hashiguchi, K., Obinata, M., Yamasaki, M., and Tamura, G. (1986) Essential structure in the cloned transforming DNA that induces gene amplification of the *Bacillus subtilis amyE-tmrB* region. *J. Bacteriol.* **166**, 787–794
29. Amano, H., Ives, C.L., Bott, K.F., and Shishido, K. (1991) A limited number of *Bacillus subtilis* strains carry a tetracycline-resistance determinant at a site close to the origin of replication. *Biochim. Biophys. Acta* **1088**, 251–258
30. Itaya, M. and Tanaka, T. (1999) Fate of unstable *Bacillus subtilis* subgenome: re-integration and amplification in the main genome. *FEBS Lett.* **448**, 235–238
31. Westers, H., Dorenbos, R., van Dijl, J.M., Kabel, J., Flanagan, T., Devine, K.M., Jude, F., Seror, S.J., Beekman, A.C., Darmon, E., Eschevins, C., de Jong, A., Bron, S., Kuipers, O.P., Albertini, A.M., Antelmann, H., Hecker, M., Zamboni, N., Sauer, U., Bruand, C., Ehrlich, D.S., Alonso, J.C., Salas, M., and Quax, W.J. (2003) Genome engineering reveals large dispensable regions in *Bacillus subtilis*. *Mol. Biol. Evol.* **20**, 2076–2090
32. Ara, K., Ozaki, K., Nakamura, K., Yamane, K., Sekiguchi, J., and Ogasawara, N. (2007) *Bacillus* minimum genome factory: effective utilization of microbial genome information. *Biotechnol. Appl. Biochem.* **46**, 169–178
33. Rocha, E.P. (2004) The replication-related organization of bacterial genomes. *Microbiology* **150**, 1609–1627
34. Hughes, D. (1999) Impact of homologous recombination on genome organization and stability. in *Organization of the Prokaryotic Genome* (Robert, L.C., ed.) pp. 109–128 ASM Press, Washington, DC
35. Ohashi, Y., Ohshima, H., Tsuge, K., and Itaya, M. (2003) Far different levels of gene expression provided by an oriented cloning system in *Bacillus subtilis* and *Escherichia coli*. *FEMS Microbiol. Lett.* **221**, 125–130